Astronomy
&
Astrophysics

Spectral types and masses of white dwarfs in globular clusters[*],[**],[***]

S. Moehler[1,4], D. Koester[1], M. Zoccali[2,5], F. R. Ferraro[3], U. Heber[4], R. Napiwotzki[4], and A. Renzini[5]

[1] Institut für Theoretische Physik und Astrophysik der Universität Kiel, 24098 Kiel, Germany
   e-mail: koester@astrophysik.uni-kiel.de
[2] Departamento de Astronomía y Astrofísica, Pontificia Universidad Católica de Chile, Avenida Vicuña Mackenna 4860,
   782-0436 Macul, Santiago, Chile
   e-mail: mzoccali@astro.puc.cl
[3] Dipartimento di Astronomia, Università di Bologna, via Ranzani 1, 40127 Bologna, Italy
   e-mail: ferraro@bo.astro.it
[4] Dr. Remeis-Sternwarte, Astronomisches Institut der Universität Erlangen-Nürnberg, Sternwartstr. 7,
   96049 Bamberg, Germany
   e-mail: heber@sternwarte.uni-erlangen.de;rn38@astro.le.ac.uk
[5] European Southern Observatory, Karl Schwarzschild Strasse 2, 85748 Garching bei München, Germany
   e-mail: arenzini@eso.org

Abstract. White dwarfs in globular clusters offer additional possibilities to determine distances and ages of globular clusters, provided their spectral types and masses are known. We therefore started a project to obtain spectra of white dwarfs in the globular clusters NGC 6397 and NGC 6752. All observed white dwarfs show hydrogen-rich spectra and are therefore classified as DA. Analysing the multi-colour photometry of the white dwarfs in NGC 6752 yields an average gravity of $\log g = 7.84$ and 0.53 $M_\odot$ as the most probable average mass for globular cluster white dwarfs. Using this average gravity we try to determine independent temperatures by fitting the white dwarf spectra. While the stellar parameters determined from spectroscopy and photometry usually agree within the mutual error bars, the low resolution and S/N of the spectra prevent us from setting constraints stronger than those derived from the photometry alone. For the same reasons the white dwarf spectra obtained for NGC 6397 unfortunately do not provide an independent distance estimate of sufficient accuracy to distinguish between the long and short distance scale for globular clusters.

Key words. stars: white dwarfs – Galaxy: globular clusters: individual: NGC 6397 – Galaxy: globular clusters: individual: NGC 6752

1. Introduction

As white dwarfs are the final stage in the evolution of all low mass stars, many are expected to exist in globular clusters. However, due to their faintness and occurrence in very crowded fields they were detected only after the refurbishment of HST with the WFPC2. Several candidate white dwarfs were then soon identified in M 15 (de Marchi & Paresce 1995), ω Cen

(Elson et al. 1995), NGC 6397 (Paresce et al. 1995a; Cool et al. 1996), M 4 (Richter et al. 1995, 2002), 47 Tuc (Paresce et al. 1995b; Zoccali et al. 2001) and NGC 6752 (Renzini et al. 1996). Renzini & Fusi Pecci (1988) suggested to use the white dwarf sequence as a standard candle for determining the distance to nearby globular clusters, similarly to the traditional main sequence fitting procedure using local subdwarfs with known trigonometric parallax. In this case, the white dwarf sequence of the cluster is compared to a sequence constructed with local white dwarfs with accurate trigonometric parallax. The method was then applied to NGC 6752 (Renzini et al. 1996) and 47 Tuc (Zoccali et al. 2001, where also the result from Renzini et al. 1996 for NGC 6752 was updated). However, while the updated distance modulus for NGC 6752 agrees well with all other distance determinations for this cluster, the white dwarf distance to 47 Tuc is considerably shorter than that found by Gratton et al. (1997, 2003) via main sequence fitting.

While it may seem strange to use the faintest objects in a globular cluster to derive its distance, white dwarfs offer some advantages as standard candles when compared to main sequence stars:

– they come in just two varieties – either hydrogen-rich (DA) or helium-rich (DB) – *independent of their original metallicity* and, in both cases, their atmospheres are virtually free of metals. So, unlike in the case of main sequence fitting, one does not have to find local calibrators with the same metallicity as the globular clusters;

– white dwarfs are locally much more numerous than metal-poor main sequence stars and thus make it possible to define a better reference sample.

However, the method has its own specific problems, which are discussed in great detail in Zoccali et al. (2001) and Salaris et al. (2001). Indeed, the location of the white dwarf cooling sequence depends on:

– *the white dwarf mass*
On theoretical grounds, given the observed maximum luminosity reached on the asymptotic giant branch (AGB), the mass of currently forming white dwarfs in globular clusters should be $0.53 \pm 0.02 \, M_\odot$ (Renzini & Fusi Pecci 1988; Renzini et al. 1996). Unfortunately, there are no local white dwarfs in this mass range with directly determined masses (i.e. without using a mass-radius relationship). There is, however, a handful of local white dwarfs with spectroscopically determined masses near this value (cf. Table 1 in Zoccali et al. 2001), which allows the construction of a semi-empirical cooling sequence for $M_{\mathrm{WD}} = 0.53 \, M_\odot$, once relatively small mass-dependent corrections are applied to each local white dwarf. The spectroscopic determination of the masses of white dwarfs in a globular cluster was first attempted by Moehler et al. (2000) for white dwarfs in NGC 6397. However, the low S/N of the spectra of these very faint stars did not allow us to determine the mass with sufficient accuracy.

– *the white dwarf envelope mass*
In the case of DA white dwarfs the cooling sequence location depends also on the mass of the residual hydrogen-rich envelope. This affects *spectroscopically* derived masses (see above), with the resulting mass being $\approx 0.04 \, M_\odot$ higher when using the *evolutionary* envelope mass ($\approx 10^{-4} \, M_{\mathrm{WD}}$, Fontaine & Wesemael 1997) as opposed to virtually zero envelope mass. This mass uncertainty corresponds to an uncertainty of $0^{\mathrm{m}}1$ in the distance modulus and $1-1.5$ Gyr in the age derived from the main sequence turnoff.

– *spectral type*
DB stars are fainter than DA stars at a given colour, with the offset depending on the filter combination (i.e. the offset is greater in V vs. $B - V$ than in I vs. $V - I$). However, more massive DA white dwarfs are also fainter at a given colour.

The white dwarf sequence also provides a possibility to determine the age of a globular cluster if its faint end is detected. In that case one can derive the age of the globular cluster from the luminosity of its oldest and faintest white dwarfs. Aside

Table 1. Description of the used photometric data sets. The filter name, the number of exposures and the total integration time (in seconds) are given.

Filter	No. of exp.	Exp. time
F336W	12	26 400
F439W	5	10 000
F555W	5	6000
F814W	7	7000

from the observational difficulties and the uncertainties in the cooling tracks (see Chabrier et al. 2000 for more details) any error in the assumed mass affects the result. Recent very deep HST observations allowed the detection of the white dwarf cooling sequence in M 4 to unprecedented depths of $V \approx 30$ (Richer et al. 2002). As a preliminary result Hansen et al. (2002) derive an age of 12.7 ± 0.7 Gyr from the white dwarf luminosity function of M 4, consistent with other independent age estimates (their error bar, however, does not include errors due to the uncertainty of the white dwarf mass). Their result has recently been questioned by de Marchi et al. (2003), who claim that the cluster membership of the white dwarfs can not be verified down to sufficiently faint limits to obtain more than a lower limit of the age. Richer et al. (2004) showed, however, that different methods of data reduction and analysis account for the different depths reached with the same data and thereby defended the original result of Hansen et al. (2002).

In view of the relevance of the white dwarf masses and spectral types to the problems described above we decided to observe spectra of white dwarfs in NGC 6397 and NGC 6752 to determine their spectral types and obtain mass estimates. Pilot observations of the white dwarf candidates in NGC 6397 (63.H-0348) had already shown that the targets are hydrogen-rich DA white dwarfs (Moehler et al. 2000), but did not permit much quantitative work.

2. Observations and data reduction

2.1. Photometry

The dataset used for NGC 6752 in the present work consists of a series of HST/WFPC2 exposures taken through the filters *F336W*, *F439W*, *F555W*, *F814W* in March and April 1995 as a part of the HST programme GO5439 (see Table 1). Results based on this dataset have been already published in Renzini et al. (1996) and Ferraro et al. (1997). The field is centered about $2'$ south-east of the cluster center (see Fig. 1 in Ferraro et al. 1997).

All the photometric reductions have been carried out using ROMAFOT (Buonanno et al. 1983), a package specifically developed to perform accurate photometry in crowded fields. A version of ROMAFOT optimized to handle sub-sampled HST images has been used for the present work (see Buonanno & Iannicola 1988). Details of the reduction procedure can be found in Ferraro et al. (1997). In short, we combined all the images in each filter obtaining a median image free of cosmic ray events and other defects. To perform a deep search for

Table 2. The photometric data for the twelve most isolated white dwarfs in NGC 6752 in the Vega-based HST flight system.

Star	U_{336}	ΔU_{336}	B_{439}	ΔB_{439}	V_{555}	ΔV_{555}	I_{814}	ΔI_{814}
WF2-241	$24\overset{m}{.}014$	$0\overset{m}{.}040$	$25\overset{m}{.}052$	$0\overset{m}{.}020$	$24\overset{m}{.}818$	$0\overset{m}{.}030$	$24\overset{m}{.}916$	$0\overset{m}{.}060$
WF2-3648	$22\overset{m}{.}919$	$0\overset{m}{.}020$	$24\overset{m}{.}152$	$0\overset{m}{.}020$	$24\overset{m}{.}119$	$0\overset{m}{.}030$	$24\overset{m}{.}195$	$0\overset{m}{.}040$
WF2-5639	$21\overset{m}{.}707$	$0\overset{m}{.}010$	$23\overset{m}{.}261$	$0\overset{m}{.}020$	$23\overset{m}{.}281$	$0\overset{m}{.}020$	$23\overset{m}{.}447$	$0\overset{m}{.}030$
WF3-296	$24\overset{m}{.}493$	$0\overset{m}{.}080$	$25\overset{m}{.}419$	$0\overset{m}{.}020$	$25\overset{m}{.}287$	$0\overset{m}{.}040$	$24\overset{m}{.}770$	$0\overset{m}{.}070$
WF3-1610	$23\overset{m}{.}004$	$0\overset{m}{.}030$	$24\overset{m}{.}321$	$0\overset{m}{.}020$	$24\overset{m}{.}212$	$0\overset{m}{.}020$	$24\overset{m}{.}127$	$0\overset{m}{.}030$
WF3-3584	$23\overset{m}{.}718$	$0\overset{m}{.}040$	$24\overset{m}{.}908$	$0\overset{m}{.}020$	$24\overset{m}{.}632$	$0\overset{m}{.}020$	$24\overset{m}{.}639$	$0\overset{m}{.}040$
WF3-4909	$24\overset{m}{.}256$	$0\overset{m}{.}070$	$25\overset{m}{.}295$	$0\overset{m}{.}020$	$25\overset{m}{.}020$	$0\overset{m}{.}040$	$24\overset{m}{.}923$	$0\overset{m}{.}050$
WF3-6441	$23\overset{m}{.}577$	$0\overset{m}{.}040$	$24\overset{m}{.}574$	$0\overset{m}{.}020$	$24\overset{m}{.}480$	$0\overset{m}{.}030$	$24\overset{m}{.}613$	$0\overset{m}{.}040$
WF3-6454	$23\overset{m}{.}750$	$0\overset{m}{.}050$	$24\overset{m}{.}895$	$0\overset{m}{.}020$	$24\overset{m}{.}628$	$0\overset{m}{.}040$	$24\overset{m}{.}266$	$0\overset{m}{.}060$
WF4-1700	$22\overset{m}{.}983$	$0\overset{m}{.}030$	$24\overset{m}{.}210$	$0\overset{m}{.}020$	$24\overset{m}{.}100$	$0\overset{m}{.}020$	$24\overset{m}{.}067$	$0\overset{m}{.}040$
WF4-2003	$23\overset{m}{.}733$	$0\overset{m}{.}040$	$24\overset{m}{.}730$	$0\overset{m}{.}020$	$24\overset{m}{.}450$	$0\overset{m}{.}030$	$24\overset{m}{.}577$	$0\overset{m}{.}030$
WF4-2081	$23\overset{m}{.}397$	$0\overset{m}{.}040$	$24\overset{m}{.}520$	$0\overset{m}{.}020$	$24\overset{m}{.}370$	$0\overset{m}{.}020$	$24\overset{m}{.}522$	$0\overset{m}{.}040$

faint blue objects we used the combined *F439W* image (with an equivalent total exposure time of 10 000 s) as the reference frame for object detection. The object list derived from the median *F439W* image was used as input for the photometry of the median images in the other filters, and preliminary colour-magnitude diagrams (CMDs) have been obtained. The preliminary CMDs have been used to select a list of objects that fell outside the main CMD sequences. A visual inspection revealed that most of them were spurious objects (e.g., artifacts due to the diffraction patterns of bright saturated stars, hot pixels, etc.). By using the *cleaned* object list, the standard PSF fitting procedure was finally performed on each single image by using a Moffat (1969) function plus a numerical map of residuals in order to better account for the contribution of the stellar PSF wings.

A final catalogue was then compiled with coordinates and instrumental magnitudes for each star in each filter. The magnitudes were calibrated to the HST flight system following Dolphin (2000). Specifically, we applied:

1. the charge transfer efficiency (CTE) correction, which is negligible for the brightest white dwarfs, but reaches up to $0\overset{m}{.}25$ for the faintest ones in the *F336W* filter;
2. the aperture corrections, computed by means of a sample of isolated stars in each WFPC2 chip and filter, in order to ensure that the instrumental magnitudes refer to the counts in a $0\overset{''}{.}5$ radius around each star;
3. the gain correction, due to the fact that the four WFPC2 chips do not have identical response factors;
4. a correction to the U magnitude, removing the effect of the decreasing UV sensitivity of the CCD;
5. the flight system zero points, given in Table 6 of Dolphin (2000).

The resulting colour-magnitude diagram is shown in Fig. 1 and clearly shows the white dwarf sequence. The photometric data for the twelve most isolated white dwarfs in NGC 6752, from which the spectroscopic targets were selected, are listed in Table 2.
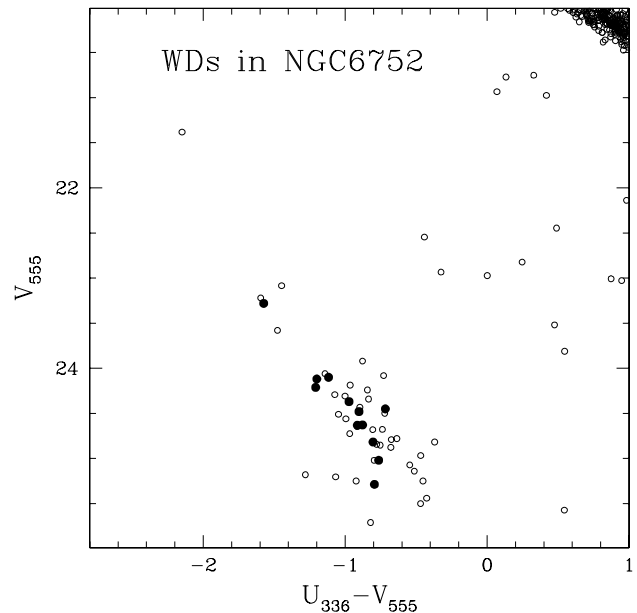
Fig. 1. V vs. $U - V$ (Vega-based flight system) for the stars in NGC 6752. The stars listed in Table 2 targets are marked by filled circles.

2.2. Spectroscopy

The spectroscopic targets in NGC 6397 (65.H-0531(B)) were selected from the photometry by Cool et al. (1996), those in NGC 6752 (67.D-0201(B)) from the data discussed in Sect. 2.1. We took care to select stars as isolated as possible to avoid contamination from neighbouring stars. The spectra were obtained in service mode with FORS1 at VLT-UT1 (Antu) and VLT-UT3 (Melipal) on the dates given in Table 3 (available in electronic form at EDP Sciences, Table 3 contains information on the observation dates, airmasses, moon and seeing conditions). We used the MOS mode of FORS1 (slit length 19″) with the high resolution collimator ($0\overset{''}{.}1$/pixel), a slit width of $0\overset{''}{.}8$ and grism V300. The detector was a TK2048EB4-1 backside thinned CCD with 2048×2048 pixels of $(24\,\mu m)^2$, which
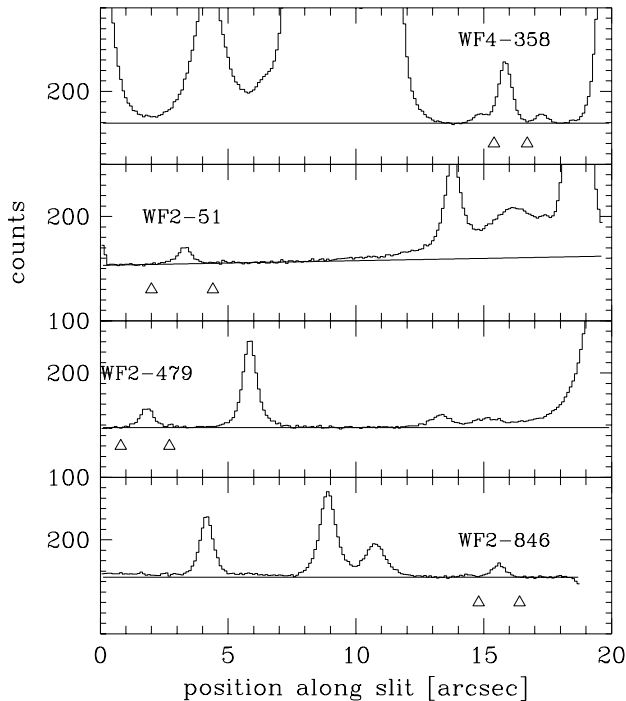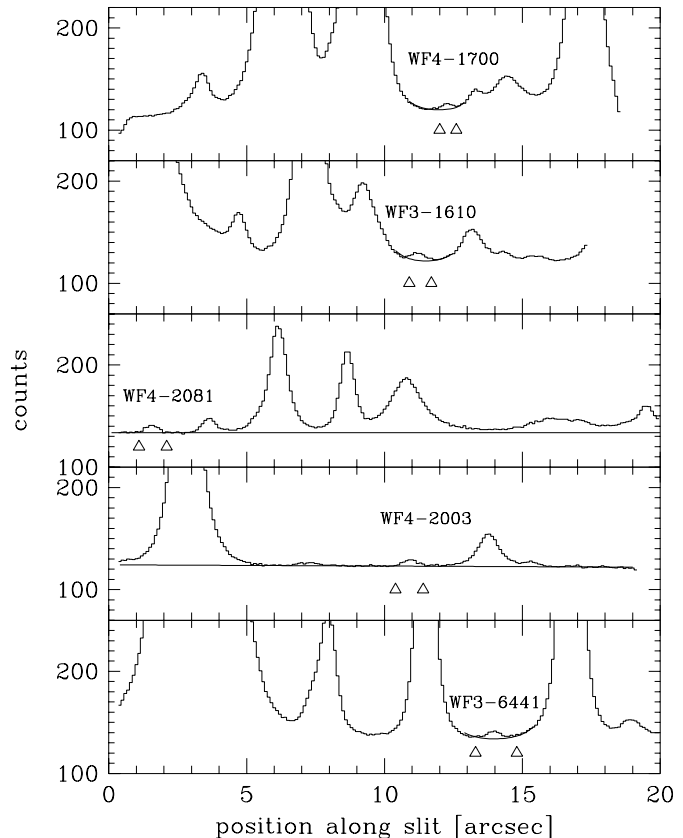
Fig. 2. Spatial brightness profile of the stars observed in NGC 6397 for each slitlet. The histogram profiles were obtained by averaging the two-dimensional spectra between 4000 Å and 5000 Å. The straight lines mark the profile of the fitted sky background averaged over the same wavelength range. The triangles mark the spatial range over which the white dwarf spectra were extracted.

Fig. 3. Spatial brightness profile of the stars observed in NGC 6752 for each slitlet. The profiles were obtained by averaging the two-dimensional spectra (histograms) respectively the two-dimensional fitted background (smooth lines) between 4000 Å and 5000 Å. The slitlets containing WF3-6441, WF3-1610, and WF4-1700 clearly show the effect of light from neighbouring stars providing a spatially varying background at the white dwarf's position. The triangles mark the spatial range over which the white dwarf spectra were extracted.

was read out with high gain (1.46 e⁻/count, 5.15 e⁻ read-out noise, NGC 6397) respectively low gain (2.87 e⁻/count, 6.07 e⁻ read-out noise, NGC 6752) and normal read-out speed using one read-out port only. This configuration yields a reciprocal dispersion of 2.5 Å/pixel and a wavelength coverage of at least 3500 Å to 5700 Å (depending on the position of the slitlet, larger coverage is also possible).

The slit width is larger than the requested seeing of 0″.6 to tolerate small positioning inaccuracies, but results in a seeing-dependent resolution in those cases where the actual seeing is smaller than the slit width (cf. Table 3). As discussed below, due to the low resolution and S/N of our spectra the change in resolution due to varying seeing does not affect the results of the spectral fitting. As FORS1 is equipped with an atmospheric dispersion corrector MOS observations at higher airmass are not a problem.

The spectra were supposed to be observed only if the seeing was better than 0″.6 (corresponding to a resolution of 15 Å). However, due to the faintness of our targets we had to use rather long exposure times (2955 s for NGC 6397 and 4380 s for NGC 6752), during which the seeing might have changed. A few exposures were stopped before reaching the requested exposure time due to technical problems. The values provided in Table 3 are averaged over the exposure time unless noted otherwise. Some spectra were taken at too bad seeing (≥1″) or with rather bright and nearby moon. Those observations provided no useful data and are therefore not listed in Table 3.

For NGC 6752 dome flat fields with two different illumination patterns were observed for each night. For the previous programme on NGC 6397, however, we had dome flat fields (again with two different illumination patterns) only for the nights of July 3, 8, and 24, 2000. For data from the other nights we used the flat field closest in time. As part of the standard calibration we were also provided with masterbias frames for our data. The masterbias showed no evidence for hot pixels and was smoothed with a 30 × 30 box filter to keep any possible large scale variations, but erase noise. The flat fields were averaged for each night and bias-corrected by subtracting the smoothed masterbias of the night. From the flat fields we determined the limits of the slitlets in spatial direction. Each slitlet was extracted and from there on treated like a long-slit spectrum. The flat fields were normalized along the dispersion axis with a linear fit, which corrected most of the large scale variations.

Due to the low resolution of the data we obtained a wavelength calibration spectrum with a slit width of 0″.3 (the center positions of the slitlets were unchanged) to allow a better definition of the line positions. The dispersion relation for all spectra was obtained from this one calibration spectrum by fitting 3rd or 4th order polynomials along the dispersion axis.

We used 13 to 16 unblended lines between 3600 Å and 6200 Å and achieved an r.m.s. error of about 0.1 Å per CCD row.

Due to the long exposure times the scientific observations contained a large number of cosmic ray hits. Those were corrected with the algorithm described in Gössl & Riffeser (2002), using a threshold of 15σ and a *FWHM* of 1.5 pixels for the cosmic ray hits. As the routine is not intended originally for the use with spectra we also reduced the uncleaned frames to allow a check for any possible artifacts of the cosmic cleaning procedure, but found none. The slitlets with the stellar spectra were extracted in the same way as the flat field and wavelength calibration slitlets. The smoothed masterbias was subtracted and they were divided by the corresponding normalized flat fields, before they were rebinned to constant wavelength steps.

For the NGC 6397 data we then filtered the rebinned frames along the spatial axis with a median filter of 7 pixels (corresponding to 0″.7) width to erase any remaining cosmic ray hits and reduce the noise in the sky background. We then identified regions uncontaminated by any stellar source in the filtered data (where the profiles of the stars are of course widened) and approximated the spatial distribution of the sky background by a constant or a linear fit (cf. Fig. 2). The sky background spectra obtained this way from the filtered data were then subtracted from the *unfiltered* two-dimensional spectra.

In the case of NGC 6752 three of the observed regions (WF4-1700, WF3-1610, and WF3-6441) were so crowded that the wings of spectra of brighter stars contributed to the background of the white dwarf spectra (cf. Fig. 3). To account for this varying background we fitted the wings of the brighter stars with Lorentzian profiles. The *FWHM* and position of the two Lorentzian profiles were determined from averaged spatial profiles like those shown in Fig. 3 and the maximum was varied with wavelength to account for the spectral features of the bright stars. For WF4-2081 and WF4-2003 we performed the sky background subtraction in the same way as described for NGC 6397.

For both clusters the sky-subtracted spectra were extracted using Horne's (1986) algorithm as implemented in MIDAS (Munich Image Data Analysis System). Finally the spectra were corrected for atmospheric extinction using the extinction coefficients for La Silla (Tüg 1977) as implemented in MIDAS. As can be seen from Table 3 we observed a large number of spectra for each target, which had to be co-added. Before averaging the spectra for each star we had to ensure that they are all on the same wavelength scale. As the wavelength calibration spectra are obtained during daytime slight shifts between the slitlet positions of scientific and calibration observations may occur. Due to their very low S/N we cannot check for offsets using the individual white dwarf spectra themselves. To account for possible zero-point shifts in wavelength we cross-correlated the range 5500 Å–5650 Å in the sky background spectra of all scientific observations with the first spectra obtained on the night of June 30, 2000 (NGC 6397) and August 13, 2001 (NGC 6752). If the mean shift for all spectra from one exposure was more than 0.5 Å (corresponding to 0.2 pixels) we corrected all spectra from that exposure with the mean offset. This correction however, cannot account for small offsets of the stars' positions from the center of the slit in the dispersion direction.
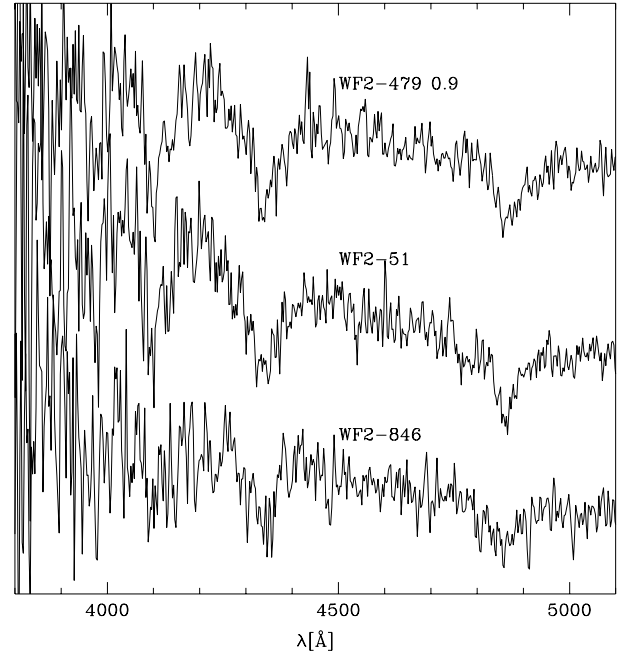

Fig. 4. Spectra of the three fainter white dwarfs in NGC 6397.

The signal-to-noise ratio of the individual spectra was much too low to obtain these offsets via radial velocities at a resolution of about 15 Å. For the stars in NGC 6752 we were lucky to have a blue horizontal branch star in one of the slitlets. We used the spectrum of this star to determine any remaining velocity shifts and used those to correct the spectra of the white dwarfs to laboratory wavelengths. In NGC 6397 we used the radial velocity offset derived from the spectrum of WF4-358 for each observation to correct all other spectra.

For a relative flux calibration we used response curves derived from spectra of LTT 6248, LTT 7987, and LTT 9239 with the data of Hamuy et al. (1992) for NGC 6752. For NGC 6397 we used the standard stars LTT 7379, Feige 110 (Hamuy et al. 1992) and GD 248 (Oke 1990). The response curves were fitted by splines and averaged for all nights. The white dwarf spectra of NGC 6752 were normalized with a curve fitted to the continuum of the blue HB star spectrum, which had also been used for the determination of the velocity shifts. The resulting spectra are shown in Figs. 4–6, with the brightness of the stars decreasing from top to bottom. The region below 3800 Å is completely dominated by noise, so that neither a spectral slope nor spectral lines can be identified. This may be explained by the low UV throughput of FORS1, the reasons for which are not understood. Also the brightest star, WF4-358, however, shows no spectral lines below 3800 Å.

3. Fit of the photometry of NGC 6752

3.1. Theoretical magnitudes for the HST photometry

To calculate theoretical magnitudes in the so called "STMAG" system of the WFPC2 (Holtzman et al. 1995) we used the grid
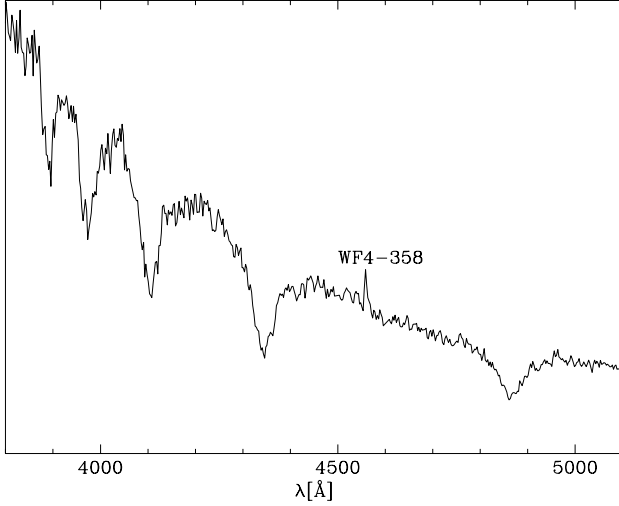
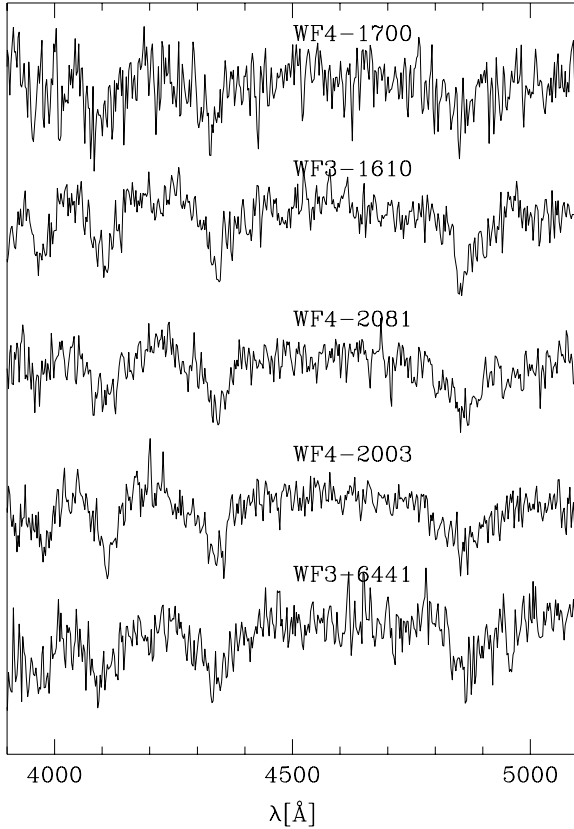**Fig. 5.** Spectrum of the brightest white dwarf observed in NGC 6397.

Fig. 6. Spectra of the white dwarfs in NGC 6752 (normalized).

of DA model atmospheres of Koester (see Finley et al. 1997 for a detailed description) and the following definition of M_{STMAG}

$$M_{\text{STMAG}} = -2.5 \frac{\int S(\lambda)F_\lambda \, d\lambda}{\int S(\lambda) \, d\lambda} - 21.1$$

where $S(\lambda)$ is the filter response function and F_λ is the mean intensity of the stellar disk or $4H_\lambda$ in terms of the Eddington flux. Note that M_{STMAG} is not an absolute magnitude but is used to distinguish theoretical from observed magnitudes m. With this

definition of STMAG the magnitudes are all zero ($M_{\text{STMAG}} = 0$) for a star with a constant F_λ of 3.63×10^{-9} erg s^{-1} cm^{-2} Å^{-1}.

A star observed in this system should have magnitude $m_{\text{STMAG}} = 0$, if the flux arriving at the earth is $f_\lambda = 3.63 \times 10^{-9}$ in the same units. The relation between observed and theoretical magnitude can be obtained from

$$f_\lambda = \frac{\pi R^2}{d^2} F_\lambda$$

$$m_{\text{STMAG}} = -2.5 \log \frac{\pi R^2}{d^2} + M_{\text{STMAG}} + 21.1$$

$$= M_{STMAG} + (m - M) - 5 \log \frac{R}{R_\odot} + 41.991,$$

here, R is the radius of the star, d the distance, and $(m - M)$ the apparent distance modulus for the respective filter band.

The observed magnitudes for the white dwarfs in the globular clusters were not determined in the STMAG system, but rather in the so called "WFPC2 Flight System" (Holtzman et al. 1995; Dolphin 2000). We have chosen to transform the observations to the STMAG system by applying the difference between the two zero points (STMAG from Holtzman et al. 1995 and FS from Dolphin 2000) before the fitting. The applied corrections (STMAG-FS) are $0.^{\text{m}}128$, $-0.^{\text{m}}724$, $-0.^{\text{m}}041$, $1.^{\text{m}}228$ for the magnitudes $U_{336}, B_{439}, V_{555}, I_{814}$ respectively. We have tested this procedure in the following way:

First we calculated the expected magnitudes for Vega in the STMAG system, using the absolutely calibrated Vega spectrophotometry from the HST archive (Colina et al. 1996). The inverse of the above corrections were then applied to the Vega STMAG magnitudes, which should bring them on the Flight System, with the resulting values $-0.^{\text{m}}008$, $0.^{\text{m}}076$, $0.^{\text{m}}039$, $0.^{\text{m}}002$ for $U_{336}, B_{439}, V_{555}, I_{814}$. The Flight System is defined in such a way that it should match the magnitudes of the ground based system used for pre-flight calibrations for stars with zero colors (see Holtzman et al. 1995 for a detailed discussion). Vega has approximately zero colors, but the magnitudes – though coming close – do not exactly match the observed *UBVI* magnitudes, which Holtzman et al. (1995) take as $0.^{\text{m}}02$, $0.^{\text{m}}02$, $0.^{\text{m}}03$, $0.^{\text{m}}035$. One probable reason for this difference is that the calibration between flight system and ground system was built using stars (mainly white dwarfs) with a spectral type very different from that of Vega. The stars used, in fact, have much higher surface gravities and stronger Balmer lines.

Although it would be possible to make additional corrections in an attempt to bring the system of the globular cluster white dwarfs closer to the Vega system, we do not believe that this is worthwhile in view of several other calibration uncertainties and the observational errors for the faint objects.

3.2. Fitting observations with theoretical magnitudes

When trying to fit a set of observed magnitudes with theoretical values we have in principle the possibility to determine simultaneously the three parameters T_{eff}, $\log g$ and distance. Effective temperature and surface gravity determine M_{STMAG} as described above and provide the radius R of the white dwarf via the Wood (1995) mass-radius relation. In practice it turned

Table 4. Fitting the photometry of the twelve most isolated white dwarfs in NGC 6752 with T_{eff} and $\log g$ as free parameters, $(m - M)_0$ fixed at $13\overset{m}{.}05$ and $13\overset{m}{.}20$. E_{B-V} assumed as $0\overset{m}{.}04$.

Object	$(m - M)_0 = 13\overset{m}{.}05$				$(m - M)_0 = 13\overset{m}{.}20$			
	T_{eff}	ΔT_{eff}	$\log g$	$\Delta \log g$	T_{eff}	ΔT_{eff}	$\log g$	$\Delta \log g$
WF2-241	13 000	600	8.08	0.07	13 100	500	7.99	0.06
WF2-3648	17 400	500	7.94	0.04	17 500	400	7.84	0.04
WF2-5639	25 200	500	7.86	0.03	25 200	500	7.77	0.03
WF3-296	9400	1500	7.66	0.46	9400	1500	7.54	0.49
WF3-1610	16 700	1700	7.94	0.14	16 700	1700	7.84	0.15
WF3-3584	13 400	1000	8.00	0.11	13 600	1100	7.91	0.12
WF3-4909	11 300	200	8.00	0.02	11 200	300	7.90	0.05
WF3-6441	14 700	1300	7.99	0.14	14 700	1200	7.89	0.12
WF3-6454	10 400	1900	7.52	0.45	10 700	2000	7.47	0.51
WF4-1700	16 200	900	7.85	0.08	16 300	1000	7.75	0.09
WF4-2003	13 000	800	7.86	0.09	13 100	700	7.76	0.09
WF4-2081	15 300	700	7.98	0.06	15 400	600	7.88	0.05
weighted mean			7.96	0.02			7.84	0.02

out to be impossible to determine all three free parameters from only four observed magnitudes. In addition to observational errors, the major problem is the strong degeneracy with respect to the parameters. The *relative* energy distribution for the white dwarfs in the observed parameter range depends mostly on T_{eff} and only very little on $\log g$. The *solid angle* ($\pi R^2/d^2$), which determines the difference between observed and theoretical magnitudes, depends strongly on both $\log g$ (through the mass-radius relation) and on the distance. Therefore a small change in $\log g$ can be easily compensated by a change in distance and vice versa. Figure 7 shows the strong correlation between derived surface gravity and distance modulus.

It was therefore necessary to keep one or two parameters fixed at some pre-determined value to achieve a robust fitting result. The fitting used a χ^2 routine based on the Levenberg-Marquardt algorithm (Press et al. 1992), and is described in more detail in Zuckerman et al. (2003). Before the fit, the magnitudes were dereddened assuming $E_{B-V} = 0\overset{m}{.}04$, and the extinction coefficients of Holtzman et al. (1995).

We decided to keep the distance modulus fixed as it is rather well known for NGC 6752: The distance modulus obtained by Renzini et al. (1996) using white dwarfs in the cluster was $13\overset{m}{.}05$. A reevaluation of these white dwarf observations, using the "thick hydrogen envelope" models results in $13\overset{m}{.}15$ (Zoccali et al. 2001). Recent determinations with main sequence fitting obtain $13\overset{m}{.}17$ (Reid 1998) and $13\overset{m}{.}23$ (Gratton et al. 1997). Gratton et al. (2003) recently published a new distance determinations for NGC 6752 from main sequence fitting, which yielded $(m - M)_0 = 13\overset{m}{.}23$ from Johnson photometry and $(m - M)_0 = 12\overset{m}{.}99$ from Strömgren photometry. As it is unclear from their data which value is the correct one we do not use this new determination for our average distance. For our fits we have used the short distance originally determined by Renzini et al. (1996, $13\overset{m}{.}05$) as an extreme case, as well
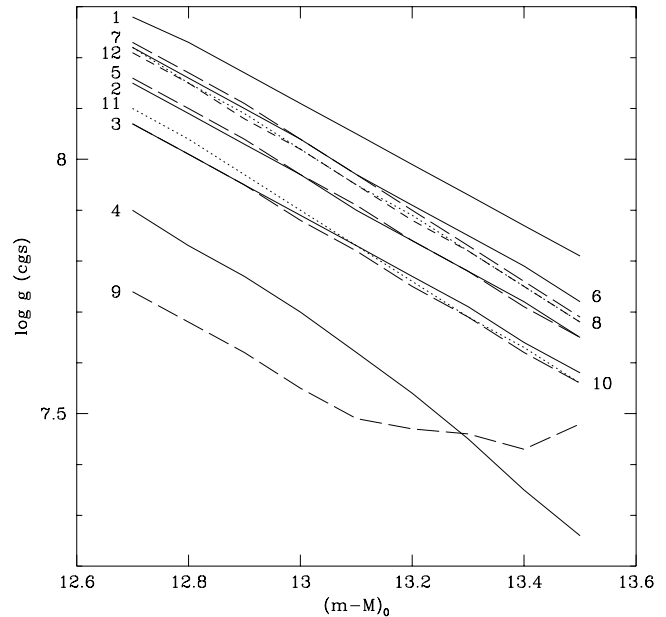
Fig. 7. Surface gravities determined from the photometric data listed in Table 4 for various distance moduli. The numbers refer to the position of the star in Table 4.

as the average of the more recent determinations not involving white dwarfs ($13\overset{m}{.}20$).

The results listed in Table 4 show that the scatter in $\log g$ is quite small due to the very strong correlation between the radius ($\log g$) and distance through the solid angle of the star (see above). The average value for the surface gravity is 7.96 for $(m-M)_0 = 13\overset{m}{.}05$ and 7.84 for $(m-M)_0 = 13\overset{m}{.}20$ with an error of the mean of 0.02. With the Wood (1995) mass-radius relation for a typical T_{eff} of 15 000 K and "thick hydrogen layer" (10^{-4} of the stellar mass) this corresponds to masses of 0.59 $M_\odot$ and 0.53 $M_\odot$, for the short and long distance modulus,

respectively. Assuming instead the more unlikely case of a "thin" hydrogen layer ($\leq 10^{-6}\ M_{WD}$) the mass would be $0.56\ M_\odot$ for $(m - M)_0 = 13^m\!05$ and $0.50\ M_\odot$ for $(m - M)_0 = 13^m\!20$. If we consider that the progenitor stars in globular clusters should have less than $1\ M_\odot$ and that NGC 6752 has an exclusively blue horizontal branch with a very extended blue tail, the smaller mass seems much more likely and gives strong support for the larger of the two distances, in agreement with most distance determinations for NGC 6752. Using the distance modulus as variable parameter and $\log g$ as fixed (7.96, 7.84) yields essentially the same results, as expected. The effective temperature of the objects does not change significantly with the various methods, and we may conclude that it is fairly well constrained.

4. Spectral fits for NGC 6752 and NGC 6397

The observed spectra for the white dwarfs in the two clusters were analysed with the same model atmosphere grid used for the calculation of the theoretical magnitudes. To verify the influence of different fit programs on the results (and thus get at least some estimate of the minimum true errors as opposed to the purely statistical errors provided by the fit routines) we used the procedure described in Finley et al. (1997, marked by "DK") and that described in Napiwotzki et al. (1999, marked by "RN").

The low S/N and resolution of the spectra leads to very large errors if T_{eff} and $\log g$ are both used as free parameters. We have therefore decided to keep $\log g$ fixed at the value 7.84 obtained as the most likely value from the photometry of NGC 6752. For the spectral fits we used a resolution of 15 Å, corresponding to a seeing of $0''\!6$ (which is the average seeing of our observations).

To allow a better understanding of our results and their errors we discuss here some technical details of the fitting procedures as applied in this case. When searching for the best-fitting model (by the χ^2 fitting routine) in a first step the model is fitted to the observations at pre-selected "continuum" points. In the DK fitting routine these are 7 points located in the continuum between H_γ and H_β and longward of H_β in the red part of the spectrum, and in the middle between Balmer lines in the blue part. The observed continuum is determined from the median of the flux in a region $20-100$ Å wide around these points. For each of these continuum wavelengths a normalizing factor is calculated, which would adjust the model flux to the observations at these points. The complete normalized model spectrum is then obtained by interpolating these normalization factors. Since this uses a linear interpolation the normalized model can show abrupt changes in slope from one interval to the next if the observation is badly calibrated or extremely noisy, as is apparent at the blue ends of some of the spectra in Figs. 8 and 9. After this normalization the χ^2 is determined from the comparison of model and observations in several predetermined intervals, which normally include the spectral line profiles. In the present case we have used the two intervals from $3870-4480$ and $4710-5100$ Å. These are the intervals plotted in the figures; the pure continuum region between 4480 and 4710 Å does not
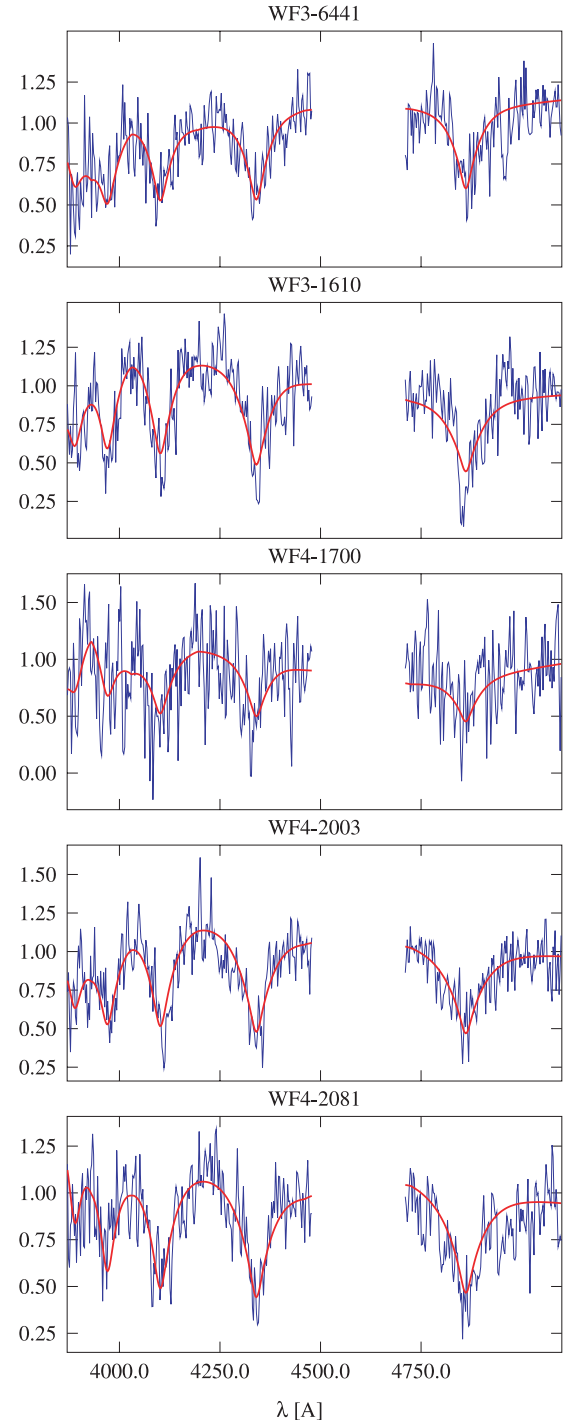
Fig. 8. Spectral fits of the white dwarfs in NGC 6752. Only the part of the spectrum which was actually fitted is shown.

contain any useful information since the normalization always forces agreement.

The major difference between the DK and the RN method is the definition of the continuum points. RN used two continuum regions of 40 Å width adjacent to the fitted regions of the H_β, H_γ, and H_δ lines. As in the DK-case, normalization factors between model and observed flux are computed and linearly interpolated for each individual Balmer line. Since the high noise level combined with the strong overlapping of the
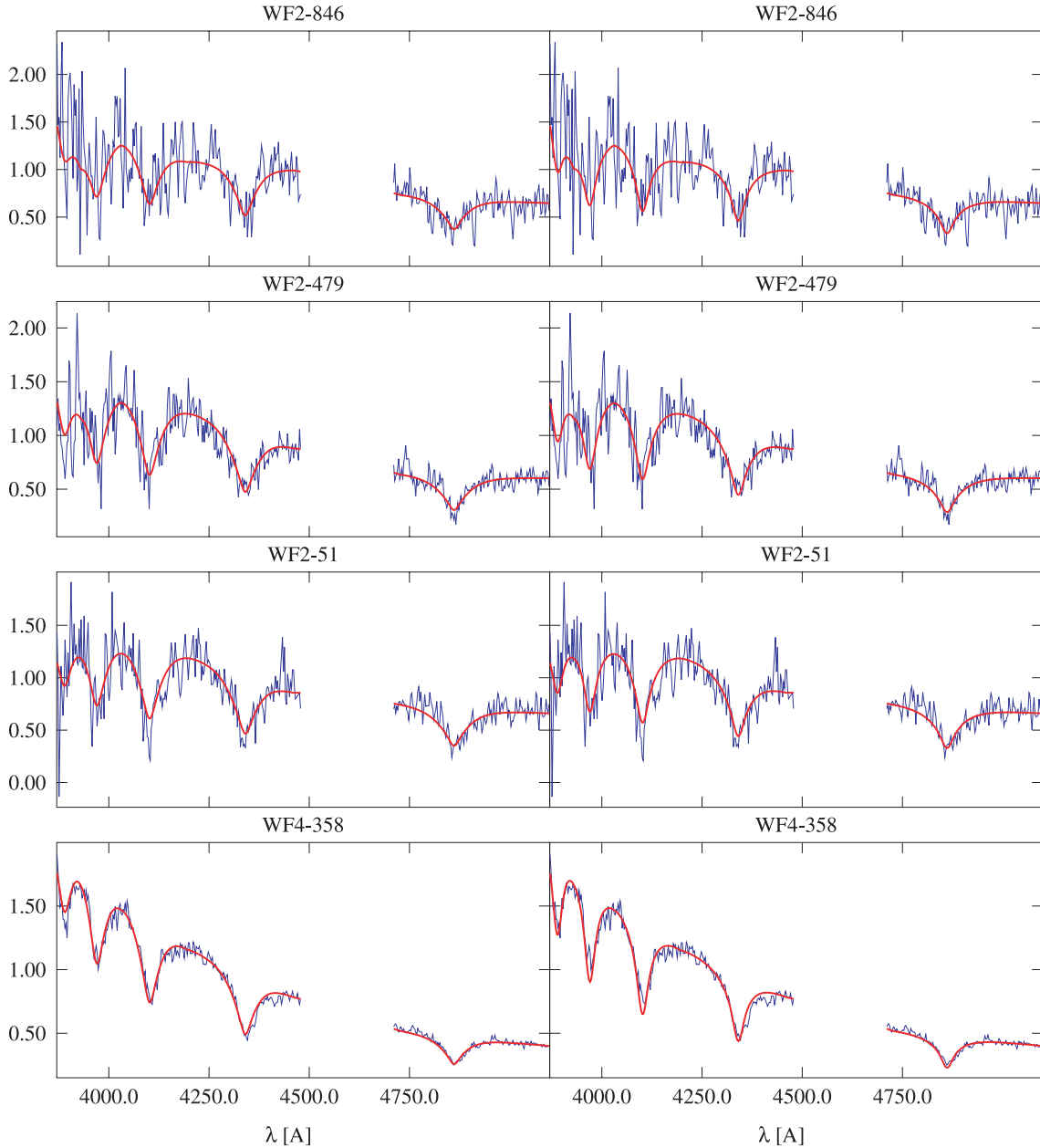
Fig. 9. Spectral fits of the white dwarfs in NGC 6397. Only the part of the spectrum which was actually fitted is shown. The *left panels* show the hot solutions, the *right panels* show the cool solutions.

lines makes the definition of continuum points between lines more and more difficult for the higher members of the Balmer series, the normalization of the region shortward of and including H_ϵ was done for all lines simultaneously. Four continuum regions (of 30 Å width) were defined from the red wing of H_ϵ to 3815 Å. A linear fit of the resulting normalization factors was performed and applied to the fitted lines.

Finally, the best-fitting model is in both cases found by minimizing χ^2 as a function of the model parameters $\log g$ and $T_{\rm eff}$. This routine automatically determines errors for the fit parameters, which are however only statistical errors, assuming that the differences between the model and the observation are caused only by statistical measurement errors distributed normally around the correct value. There are, however, a number of sources of systematic errors which cannot be

determined easily. These include the reduction procedures, with errors in our case likely being dominated by the background subtraction. It is obvious that for an observation with a background both variable and several times higher than the continuum spectrum a small error in the background determination can have a profound influence on the line profile and thus on the fitting results. Placing the continuum points differently, or interpolating the factors quadratically instead of linearly will also change the results, but without prior knowledge of the exact observed spectrum there is no reason to prefer one method over the other. Such systematic errors can only be estimated by comparing results from different spectra for the same star, or comparing results from different authors and fitting/reduction methods.

Table 5. Fitting the white dwarf spectra in NGC 6752 with log g held fixed at 7.84. $T_{\mathrm{eff,ph}}$ is the result from the photometry for $(m-M)_0 = 13\overset{\mathrm{m}}{.}20$.

Object	DK		RN			
	T_{eff}	ΔT_{eff}	T_{eff}	ΔT_{eff}	$T_{\mathrm{eff,ph}}$	$\Delta T_{\mathrm{eff,ph}}$
	[K]	[K]	[K]	[K]	[K]	[K]
WF3-1610	15 100	900	14 400[1]	1000	16 700	1700
WF3-6441	19 200	1000	21 600	1300	14 700	1200
WF4-1700	18 500	1600	16 800	1800	16 300	1000
WF4-2003	13 400	1700	13 400	2700	13 100	700
WF4-2081	12 900	800	14 600	800	15 400	600

[1] excluding the core of H$_\beta$.

Table 6. Fitting the white dwarf spectra in NGC 6397 with log g held fixed at 7.84. $T_{\mathrm{eff,ph}}$ is the effective temperature estimated from *VI* photometry by Moehler et al. (2000). We also give M_V from the model fit (assuming a thick hydrogen layer), the observed V corrected for a reddening of $E_{B-V} = 0\overset{\mathrm{m}}{.}18$, and the derived distance modulus.

Object	V_0	$T_{\mathrm{eff,ph}}$	DK				RN			
			T_{eff}	ΔT_{eff}	M_V	$(m-M)_0$	T_{eff}	ΔT_{eff}	M_V	$(m-M)_0$
		[K]	[K]	[K]			[K]	[K]		
WF2-846	$23\overset{\mathrm{m}}{.}76$	10 300	10 700	400	$11\overset{\mathrm{m}}{.}73$	$12\overset{\mathrm{m}}{.}03$	11 400	700	$11\overset{\mathrm{m}}{.}56$	$12\overset{\mathrm{m}}{.}20$
			17 900	1200	$10\overset{\mathrm{m}}{.}73$	$13\overset{\mathrm{m}}{.}03$	15 700	1000	$10\overset{\mathrm{m}}{.}96$	$12\overset{\mathrm{m}}{.}80$
WF2-479	$23\overset{\mathrm{m}}{.}33$	11 500	11 500	400	$11\overset{\mathrm{m}}{.}54$	$11\overset{\mathrm{m}}{.}79$	12 700	800	$11\overset{\mathrm{m}}{.}35$	$11\overset{\mathrm{m}}{.}98$
			15 300	600	$11\overset{\mathrm{m}}{.}01$	$12\overset{\mathrm{m}}{.}32$	14 700	800	$11\overset{\mathrm{m}}{.}07$	$12\overset{\mathrm{m}}{.}26$
WF2-51	$23\overset{\mathrm{m}}{.}46$	10 800	11 200	400	$11\overset{\mathrm{m}}{.}60$	$11\overset{\mathrm{m}}{.}86$	12 800	1000	$11\overset{\mathrm{m}}{.}34$	$12\overset{\mathrm{m}}{.}12$
			15 500	500	$10\overset{\mathrm{m}}{.}98$	$12\overset{\mathrm{m}}{.}48$	12 800	1000	$11\overset{\mathrm{m}}{.}34$	$12\overset{\mathrm{m}}{.}12$
WF4-358	$22\overset{\mathrm{m}}{.}19$	19 400	10 200	100	$11\overset{\mathrm{m}}{.}88$	$10\overset{\mathrm{m}}{.}31$	10 600	100	$11\overset{\mathrm{m}}{.}76$	$10\overset{\mathrm{m}}{.}43$
			19 000	300	$10\overset{\mathrm{m}}{.}62$	$11\overset{\mathrm{m}}{.}57$	17 900	300	$10\overset{\mathrm{m}}{.}73$	$11\overset{\mathrm{m}}{.}46$

To verify the influence of the assumed resolution on the results we also performed fits for resolution of 10 Å and 20 Å, which yielded effective temperatures hotter respectively cooler by less than 1%, which is well below even the purely statistical errors given in Table 5. The observed spectra (confined to the ranges used for the model fits) and the best fitting models for NGC 6752 are shown in Fig. 8.

The effective temperatures derived for the white dwarfs in NGC 6752 with different fit methods, although slightly different, usually agree within the errorbars (cf. Table 5) and we therefore conclude that the choice of the fit methods does not affect our results. For WF3-6441 the spectroscopic temperatures agree with each other but differ from the photometric one. This may be an effect of the rather problematic sky subtraction for this star (cf. Fig. 3 and Sect. 2.2). Despite our best efforts to approximate the spatial and spectral variation of the sky background in these crowded fields, we cannot exclude the possibility of residual background light in the extracted spectra. As the flux in the spectra is significantly lower than that of the background, small errors in the background approximation can strongly affect the spectra. We therefore rather trust the photometric results for this star, despite its larger than average error.

The observed spectra and best fitting models for the white dwarfs in NGC 6397 are shown in Fig. 9. For these stars we have only V and I photometry from Cool et al. (1996), from which we estimated temperatures in Moehler et al. (2000, cf. Table 6). These temperature estimates are very useful to distinguish between the hot and cool solutions obtained from the spectra alone (see Table 6). Based on the photometric temperature estimates we select the cool results of the spectroscopic fits for the three fainter stars and the hot result for the brightest star. As can be seen from Fig. 9 the fitted model spectra for the hot (left panel) and cool (right panel) solutions are indistinguishable by eye (except perhaps for the brightest star) and also the χ^2 values for both solutions are almost identical. As can be seen from Table 6 the cool solutions of the RN fit are hotter than those from the DK fit, whereas the situation is just the opposite for the hot solutions, indicating the presence of systematic errors in our analysis.

The parameters obtained from the spectral fit can be used to determine absolute magnitudes from the models, and – with the help of observed V values – also individual distances (see Table 6). The average distance modulus for the three fainter objects is $11\overset{\mathrm{m}}{.}9 \pm 0\overset{\mathrm{m}}{.}1$ [DK] and $12\overset{\mathrm{m}}{.}1 \pm 0\overset{\mathrm{m}}{.}1$ [RN], respectively (errors are statistical r.m.s errors only), yielding a mean distance modulus of $12\overset{\mathrm{m}}{.}0$, which is at the short end of the range of distance moduli found in the recent literature ($11\overset{\mathrm{m}}{.}99 – 12\overset{\mathrm{m}}{.}24$).

The last object – although the brightest – is rather discrepant, and may be a foreground object or have a significantly smaller log g than the others. In view of the fact that the proper

Table 7. Results for the brightest object in NGC 6397 with $\log g$ as free parameter. We also give M_V from the model fit (assuming a thick hydrogen layer), the observed V corrected for a reddening of $E_{B-V} = 0^m_{.}18$, and the derived distance modulus.

	T_{eff} [K]	ΔT_{eff} [K]	$\log g$	$\Delta \log g$	M_V	$(m-M)_0$
DK	18 800	340	7.72	0.06	$10^m_{.}47$	$11^m_{.}72$
RN	18 700	520	8.09	0.12	$11^m_{.}02$	$11^m_{.}17$

motions derived by King et al. (1998) support the cluster membership of all four white dwarfs analysed in NGC 6397 we decided to check the gravity for this star through a fit with both T_{eff} and $\log g$ as free parameters (see Table 7). Pilot spectra of this star with a combined exposure time of 1.5 h yielded an effective temperature of $18\,200 \pm 1300$ K and a surface gravity of $\log g = 7.3 \pm 0.36$ (Moehler et al. 2000). While the temperatures from all three fits agree very well, the scatter in surface gravity again shows that the systematic errors discussed above are considerably larger than the statistical ones. The lower gravity obtained by the DK fit would support the cluster membership of the brightest white dwarf, but would yield a mass of 0.48 $M_\odot$ instead of the 0.53 $M_\odot$ derived for the fainter white dwarfs in NGC 6752.

5. Conclusions

We observed a sample of white dwarfs in the globular clusters NGC 6397 and NGC 6752 and showed that they are all hydrogen-rich DA. From multicolour photometry we determined an average mass of $0.53 \pm 0.03\,M_\odot$ (uncertainty due to uncertainties of 0.02 dex in the average $\log g$ and of $0^m_{.}05$ in the distance modulus of NGC 6752). This value (based on the assumption of a thick hydrogen layer) is identical to that assumed by Renzini et al. (1996) on theoretical grounds. Therefore both observational and theoretical arguments strongly advocate against the use of 0.6 $M_\odot$ (the mean mass of the local white dwarfs) or even more for the mass of hot white dwarfs in globular clusters when comparing observations to theoretical tracks. However, the limited S/N in combination with the low resolution of the spectroscopic data prevented the independent determination of masses from spectroscopic fits alone. Multi-colour photometry may be the better way to determine the physical parameters of white dwarfs in globular clusters once their spectral types are known. For spectroscopic observations our experience shows that crowding can severely limit the usefulness of the data due to problems with sky subtraction. We would therefore strongly recommend to look for white dwarf candidates in ground-based wide-field photometry to avoid the problems we encountered for NGC 6752. Also a better sensitivity in the blue would be useful for future spectroscopy.

References

Buonanno, R., & Iannicola, G. 1988, PASP, 101, 294
Buonanno, R., Buscema, G., Corsi, C. E., Ferraro, I., & Iannicola, G. 1983, A&A, 126, 278
Chabrier, G., Brassard, P., Fontaine, G., & Saumon, D. 2000, ApJ, 543, 216
Colina, L., Bohlin, R. C., & Castelli, F. 1996, Instrument Science Report OSG-CAL-96-01
Cool, A. M., Piotto, G., & King, I. R. 1996, ApJ, 468, 655
de Marchi, G., & Paresce, F. 1995, A&A, 304, 202
de Marchi, G., Paresce, F., Straniero, O., & Prada Moroni, P. G. 2004, A&A, 415, 971
Dolphin, A. E. 2000, PASP, 112, 1397
Elson, R. A. W., Gilmore, G. F., Santiago, B. X., & Casertano, S. 1995, AJ, 110, 682
Ferraro, F. R., Carretta, E., Bragaglia, A., Ortolani, S., & Renzini, A. 1997, MNRAS, 286, 1012
Finley, D. S., Koester, D., & Basri, G. 1997, ApJ, 488, 375
Fontaine, G., & Wesemael, F. 1997, A critical look at the question of thick vs. thin hydrogen and helium envelopes in white dwarfs, in White Dwarfs, Proc. of the 10th European Workshop on White Dwarfs, ed. J. Isern, M. Hernanz, & E. Gracia-Berro, Astrophysics and Space Science Library (Dordrecht: Kluwer Academic Publishers), 214, 173
Gössl, C., & Riffeser, A. 2002, A&A, 381, 1095
Gratton, R. G., Fusi Pecci, F., Carretta, E., et al. 1997, ApJ, 491, 749
Gratton, R. G., Bragaglia, A., Carretta, E., et al. 2003, A&A, 408, 529
Hamuy, M., Walker, A. R., Suntzeff, N. B., et al. 1992, PASP, 104, 533
Hansen, B., Brewer, J., Fahlmann, G. G., et al. 2002, ApJ, 574, L155
Holtzman, J. A., Burrows, C. J., Casertano, S., et al. 1995, PASP, 107, 1065
Horne, K. 1986, PASP, 98, 609
King, I. R., Anderson, J., Cool, A. M., & Piotto, G. 1998, ApJ, 492, L37
Moehler, S., Heber, U., Napiwotzki, R., Koester, D., & Renzini, A. 2000, A&A, 354, L75
Moffat, A. F. J. 1969, A&A, 3, 455
Napiwotzki, R., Green, P. J., & Saffer, R. A. 1999, ApJ, 517, 399
Oke, J. B. 1990, AJ, 99, 1621
Paresce, F., de Marchi, G., & Romaniello, M. 1995a, ApJ, 440, 216
Paresce, F., de Marchi, G., & Jedrzejewski, R. 1995b, ApJ, 442, L57
Press, W. H., Teukolsky, S. A., Vetterling, W. T., & Flannery, B. P. 1992, Numerical Recipes (Cambridge: Cambridge University Press)
Reid, I. N. 1998, AJ, 115, 204
Renzini, A., & Fusi Pecci, F. 1988, ARA&A, 26, 199
Renzini, A., Bragaglia, A., & Ferraro, F. R., et al. 1996, ApJ, 465, L23
Richer, H. B., Fahlmann, G. G., Ibata, R. A., et al. 1995, ApJ, 451, L17
Richer, H. B., Brewer, J., Fahlmann, G. G., et al. 2002, ApJ, 574, L151
Richer, H. B., Brewer, J., Fahlmann, G. G., et al. 2004, AJ, May issue [arXiv:astro-ph/0401446]
Salaris, M., Cassisi, S., García-Berro, E., Isern, J., & Torres, S. 2001, A&A, 371, 921
Tüg, H. 1977, ESOMe, 11, 7
Wood, M. A. 1995, Theoretical White Dwarf Luminosity Functions: DA Models, in White Dwarfs, ed. D. Koester, & K. Werner, Lecture Notes in Physics (Berlin Heidelberg, New York: Springer-Verlag), 443, 41
Zoccali, M., Renzini, A., Ortolani, S., et al. 2001, ApJ, 553, 733
Zuckerman, B., Koester, D., Reid, I. N., & Hünsch, M. 2003, ApJ, 596, 477

Online Material

Table 3. Observational parameters for the spectroscopic data. On August 10, 2001, the seeing monitor did not work and the seeing was estimated from the acquisition and through-slit images.

Target	Start of observation	Exp. time	Seeing	Airmass	Moon	
		[s]			Distance	Illumination
NGC 6397	2000/07/01 03:18:24.011	2955	0″.53	1.149	147°.4	0.007
NGC 6397	2000/07/01 04:09:25.965	2955	0″.54	1.148	147°.4	0.006
NGC 6397	2000/07/05 03:44:29.402	2955	0″.72	1.146	115°.0	0.153
NGC 6397	2000/07/05 04:35:30.895	2955	0″.87	1.174	114°.5	0.156
NGC 6397	2000/07/06 05:42:39.878	2955	0″.80	1.282	102°.2	0.254
NGC 6397	2000/07/06 06:33:39.752	2955	0″.81	1.425	101°.7	0.259
NGC 6397	2000/07/08 03:49:31.331	2955	0″.56	1.151	80°.5	0.453[1]
NGC 6397	2000/07/08 04:40:30.861	2955	0″.50	1.192	80°.1	0.457[1]
NGC 6397	2000/07/25 02:52:02.328	2955	0″.53	1.156	124°.1	0.422[2]
NGC 6397	2000/07/25 03:43:02.144	2955	0″.53	1.204	124°.5	0.417[2]
NGC 6752	2001/08/09 01:16:57.397	1756	0″.67	1.260	86°.1	0.796[3]
NGC 6752	2001/08/09 01:53:59.110	1724	0″.61	1.235	86°.4	0.794[3]
NGC 6752	2001/08/10 00:57:05.415	4380	0″.63	1.263	95°.6	0.715[4]
NGC 6752	2001/08/10 02:16:43.582	2400	0″.67	1.229	96°.2	0.710[4]
NGC 6752	2001/08/11 00:30:47.431	4380	0″.65:	1.287	105°.0	0.626[5]
NGC 6752	2001/08/11 01:50:27.188	4380	0″.55:	1.235	105°.7	0.620[5]
NGC 6752	2001/08/11 03:18:27.263	4380	0″.50:	1.280	106°.3	0.613[5]
NGC 6752	2001/08/11 04:35:06.749	4380	–	1.418	106°.9	0.608[5]
NGC 6752	2001/08/22 00:53:16.938	4380	0″.70	1.237	94°.6	0.119
NGC 6752	2001/08/22 02:16:26.569	4380	0″.56	1.262	93°.9	0.124
NGC 6752	2001/09/15 00:04:58.643	4380	0″.64	1.239	132°.8	0.092
NGC 6752	2001/09/15 01:37:23.372	4380	0″.60	1.332	132°.1	0.086
NGC 6752	2001/09/18 00:25:56.746	4380	0″.65	1.257	100°.0	0.006
NGC 6752	2001/09/18 01:41:59.797	4380	0″.53	1.363	99°.3	0.007
NGC 6752	2001/09/19 00:11:09.587	4380	0″.70	1.250	88°.2	0.035

[1] Moon rise at 11:58 UT.
[2] Moon rise at 00:47 UT.
[3] Moon rise at 02:05 UT.
[4] Moon rise at 02:56 UT.
[5] Moon rise at 03:49 UT.